

# Silicon-Based Large-Area X-Ray Detectors

Philip Kaaret

*Harvard-Smithsonian Center for Astrophysics, 60 Garden St., Cambridge, MA 02138*

## Abstract.

The great success of the Rossi X-Ray Timing Explorer (RXTE) has shown that X-ray timing is an excellent tool for study of the physics of strong gravitational fields and for measurement of fundamental physical properties of black holes and neutron stars. In order to provide a qualitative advance in X-ray timing capabilities, the next generation X-ray timing mission will require an effective area near 10 square meters with sensitivity extending into the hard X-ray band an order of magnitude increase in effective area over RXTE. Achieving such a large effective area at reasonable cost will require advances in detector technology. Silicon-based detectors have a long heritage in space applications and can be fabricated in the large numbers needed for a large area detector by industry with existing facilities and at reasonable cost. I describe current work on the development of silicon-based detectors suitable for a next generation X-ray timing mission.

## GOALS FOR A FUTURE X-RAY TIMING MISSION

The primary goal of a future X-ray timing mission should be to probe extreme physical conditions in astrophysical objects including studying the behavior of matter in the strong gravitational fields around accreting objects and constraining the equation of state of ultradense matter within neutron (or quark) stars via measurement of phenomena at the stellar surface. Results from the *Rossi X-Ray Timing Explorer* (RXTE) demonstrate that the X-ray emissions from such systems contain strongly modulated signals which provide information about the physical properties of the systems. A new X-ray timing mission must sharpen our understanding of these signals so that they can be used as precise probes of fundamental physics.

The integration time required for detection of a quasi-periodic oscillation (QPO) is

$$T = 4 \frac{n_\sigma^2 \Delta\nu}{r^4 s^4} (b + s)^2$$

where  $s$  is the source counting rate,  $b$  is the background counting rate,  $\Delta\nu$  is the signal bandwidth,  $r$  is the root-mean-square (rms) amplitude of the signal, and  $n_\sigma$  is the detection significance. For bright sources, defined as sources for which the source counting rate is much larger than the background counting rate, the time for detection varies as  $T \propto 1/s^2$ . For different detectors with similar dependence of the effective area on energy, the source counting rate scales linearly with the detector area. Therefore, the time for detection of a QPO signal varies as  $T \propto 1/A^2$ , where  $A$  is the effective area. An

increase by a factor of 10 in detector effective area will lead to a decrease of two orders of magnitude in the time required for the detection of QPO signals.

This would enable a new X-ray timing mission to achieve a qualitative advance in the measurement of QPOs by permitting the detection of kHz QPOs within their coherence time. For a specific example, we take a kHz QPO detected from the accreting neutron star system 4U 1636-536 using RXTE [15]. The centroid frequency was  $\nu = 820$  Hz, the width of the QPO was  $\Delta\nu = 4$  Hz, and rms amplitude was 8%. The coherence time of this QPO, i.e. the time over which the oscillations maintain phase coherence, is  $\tau = Q/\nu$  where  $Q$  is the quality factor  $Q = \nu/\Delta\nu$ . For the measured QPO parameters, the coherence time  $\tau = 0.24$  s. The source counting rate in the Proportional Counter Array (PCA) during the QPO detection was 1700 c/s. For a new X-ray timing mission with an effective area 10 times that of the PCA and with a similar energy bandpass, the same QPO would be detected (naively applying the formula above) at  $4\sigma$  significance in 0.03 s. We conservatively use a background counting rate 30 times that of the PCA.

This QPO would be detected in a significantly shorter time interval than the coherence time of the QPO. This would open a qualitatively new window in the study of millisecond oscillations from accreting systems. Detection of the oscillations within time intervals over which they are coherent would permit identification of the mechanism of decoherence and should provide insight to their physical origin. This is a key step in understanding the QPOs so that they can be exploited as tools to study fundamental physics.

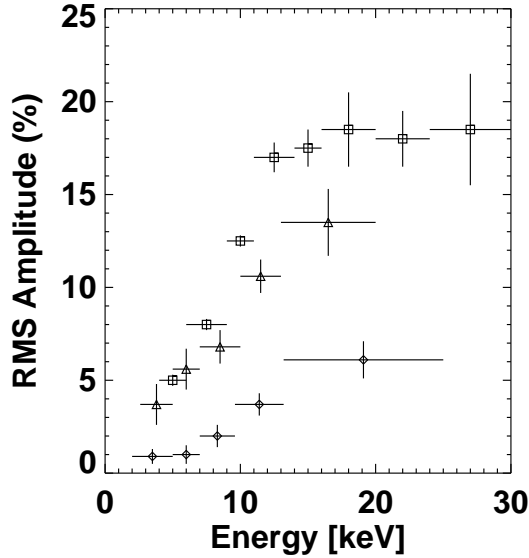


**FIGURE 1.** RMS amplitude versus energy for three typical high frequency timing signals. In all cases, the RMS amplitude increases strongly with energy. Diamonds indicate the 67 Hz QPO from GRS 1915+105 [18]. Squares indicated a kHz QPO from 4U 1608-52 [7]. Triangles indicate X-ray burst oscillations from KS 1731-260 [20].

The detection of QPOs from accreting black hole candidates (BHCs) has generated great interest, particularly because the QPO signals in most systems appear to occur at harmonically related frequencies (see the papers by Abramowicz, Remillard, and Psaltis in this volume). A key question is whether the QPO frequencies are actually constant and harmonically related or whether the frequencies drift. Our knowledge of the BHC QPOs is limited because the signals are relatively weak and, for most sources, only a few detections of the high frequency QPOs have been achieved. As an example of the effectiveness of a new X-ray timing instrument with 10 times the effective area of RXTE, we consider the detection of the 450 Hz QPO from GRO J1655-40 [24]. This was the first detection of a harmonically related, high frequency QPO signal in a BHC following the original QPO detection at 300 Hz [22]. The 450 Hz signal was detected at  $5\sigma$  significance in the 13–27 keV band in a 8164 s exposure with RXTE. For a new X-ray timing mission with an effective area 10 times that of the PCA, a background counting rate 30 times that of the PCA, and with a similar energy bandpass, the same QPO would be detected in 150 s at the same significance level. In just one observation similar to the discovery observation, the new mission would provide 50 independent measurements of the QPO and permit a sensitive search for additional harmonic structure. This would give detailed information about any potential variability in the QPO frequency. Identification of a unique model for the BHC QPOs would permit them

to be used to measure the physical parameters of the black holes such as their mass and spin.

Another RXTE discovery which offers the potential to probe fundamental physics are the quasi-periodic millisecond oscillations in X-ray bursts and the coherent millisecond pulsations from accreting neutron stars. These oscillations appear to arise from the stellar surface. Therefore, they should contain information about the surface gravity and radius of the neutron star. The ideal measurements to make would be to energy-resolved pulse profiles of individual oscillation cycles. A typical X-ray burst from the accreting neutron star and recurrent X-ray burst source 4U 1728-34 has a peak PCA counting rate of about 30,000 c/s. This source shows oscillations at a frequency of 363 Hz. A new X-ray timing mission would give 800 counts per oscillation cycle near the burst peak. Such sensitivity should lead to new constraints on the equation of state of ultradense matter.

## INSTRUMENT REQUIREMENTS

The key characteristic of RXTE is its large effective area. To achieve an order of magnitude increase in X-ray timing capabilities, a “next generation” X-ray timing mission will need a large area X-ray detector with an effective area equal to ten times that of RXTE, on the order of 6 m<sup>2</sup> [16, 5]. Good sensitivity extending up to energies of 20 to 30 keV is required because the modu-

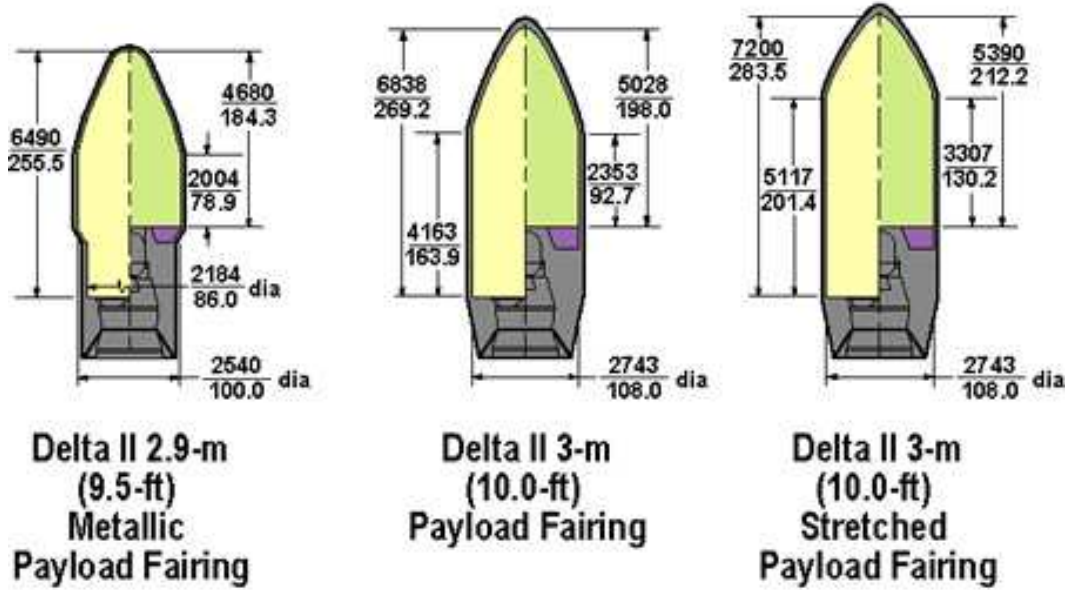


FIGURE 2. Delta II Fairings.

lation of timing signals detected from Galactic accreting objects is, in general, higher at high energies. Figure 1 shows the rms modulation versus energy for several typical high frequency signals detected with RXTE. The strong increase at high energies is clear. Because the time required for detection of a signal at fixed source counting rate scales inversely with the fourth power of the rms modulation and the detection significance for a fixed integration time scales as the square of the rms modulation, there are great advantages to be gained from a timing instrument with significant collecting area at high energies where the modulations are high. Furthermore, there are some signals, such as some of the high frequency QPOs from accreting black holes candidates discussed in the previous section that are detected only at high energies. For GRO J1655-40, the second QPO at higher frequency was detected only at energies above 13 keV [24].

Focusing of X-rays in the hard band is difficult because of the extremely small graze angles required for efficient broad-band reflection and it is unlikely that focusing telescopes will achieve the required areas, of order  $6 \text{ m}^2$ , in the near future. However, for the longer term future, microchannel plate optics offers the possibility of very light weight optics (see the contribution by Bavdaz in this volume). The Hard X-ray Telescope (HXT) on the Constellation-X mission is expected to have a total area of less than  $0.6 \text{ m}^2$  at 10 keV, and even the extended XEUS mission may achieve only  $1.7 \text{ m}^2$  at 10 keV with the area decreasing rapidly at higher energies [2]. Integrated over the band where the second QPO from GRO J1655-40 was detected, the effective area of XEUS is less than that of the RXTE PCA. While some advance in X-

ray timing will be possible with the currently planned major observatories, a significant increase in X-ray timing capabilities will likely require a dedicated mission. The detector may be non-imaging with a field of view limited by a collimator. Only moderate energy resolution ( $\sim 1 \text{ keV}$  at 6 keV) is required for most X-ray timing studies, but better energy resolution is desirable, particularly to resolve relativistically broadened Fe-K emission lines.

Non-focusing instruments do not suffer from the difficulties of reflecting hard X-ray photons and large effective area in the 10–30 keV band is relatively easily achieved. The high energy response is typically limited by absorption depth in the detector. High efficiency up to 20 or 30 keV can be achieved by deep gaseous or relatively thin solid state detectors. The primary disadvantage of a non-focusing instrument is the relatively high background counting rate. For this reason, great care must be taken to actively veto background events. Large non-focusing instruments can easily be constructed in a modular fashion. In addition to reducing costs and facilitating construction, dividing the full effective area of the instrument into multiple independent units decreases the count rate for each unit. This is particularly advantageous for a timing mission because the effect of instrumental dead time decreases, making it possible to achieve very high total count rates with minimal dead time effects. It is possible to achieve a large effective area on-orbit within the physical envelope of the Delta II launch vehicles approved for use with NASA Intermediate Explorer (MIDEX) missions, see Figure 2. If a high area efficiency can be obtained, e.g. of order 50% ratio

of effective area to detector physical area, then a detector sufficiently large for a useful new timing mission can be launched in fixed configuration in a Delta II fairing.

A large detector area with sensitivity over a broad band extending up to high energies (2-30 keV) is the critical requirement for achieving the very high source counting rate essential for the success of a future X-ray timing mission. To effectively exploit such high rates, a high telemetry bandwidth is also required. To fully telemeter the event rate of  $2 \times 10^5$  c/s from a bright source, comparable in intensity to the Crab nebula, will require a telemetry rate of the order of 10 Mbps. Multiple ground stations may be needed to achieve the required average telemetry rate. To buffer events while out of ground contact and for very bright sources, a large on-board memory (of order 100 Gbit) will be required.

Most of the sources of interest for high frequency X-ray timing are variable or transient. To maximize the scientific return of a timing mission, or timing observations in general, it is critical to have an all-sky monitor sufficiently sensitive to discover and localize new transients and determine the state of known persistent sources. In addition, flexible observation scheduling and rapid response to targets of opportunity are needed in order to perform observations while the sources are in interesting states. This is something that may be very difficult to achieve with a multi-purpose large observatory and is a strong advantage for a dedicated mission. An X-ray timing mission should be designed so that a large fraction of the sky is accessible at any instant and so that frequent repointing can be performed in order to contemporaneously monitor multiple targets.

## DETECTOR TECHNOLOGIES

The primary technology driver for a new X-ray timing mission will be the large area X-ray instrument. Here, we considered solid-state silicon detectors for the detection technology. Silicon is, perhaps, the most widely used radiation detection medium today. Silicon has a long heritage in radiation detection applications, including satellite-borne X-ray detectors which have been operated successfully in high radiation environments, e.g. [3]. Silicon detectors can be operated without high-voltage or internal amplification, and are robust and have stable operation over long periods. Furthermore, the technology for processing silicon is well understood and widely available. Hence, detectors can be fabricated by industry with existing facilities at reasonable cost and in large quantities.

The basic principle of operation of all silicon-based detectors is shown in Fig. 3. An X-ray incident on the silicon undergoes a photoelectric interaction within the

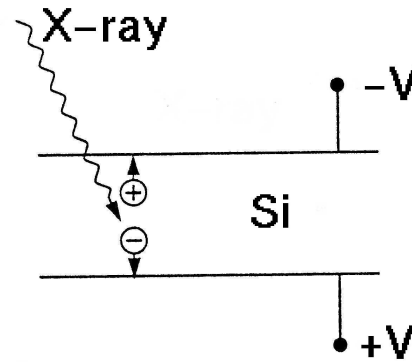


**FIGURE 3.** Basic geometry of silicon-based X-ray detector. An X-ray interacts within the silicon to produce positive and negative charge carriers with a number proportional to the incident X-ray energy. An bias voltage applied to the silicon removes free charge carriers producing a depletion region where charge carries can move freely without absorption. The same bias voltage causes the charge carrier produced by the X-ray to migrate to the boundaries of the silicon where they can be collected.

silicon releasing charge carriers. A bias voltage is applied to the silicon which removes free charge carriers from a region called the 'depletion region'. Within this region, the charge carriers produced by the X-ray can migrate freely and, due to the applied bias voltage, cause the positive and negative charge carriers to migrate in opposite directions. The charge collected at the boundary of the depletion region is proportional to the energy of the incident photon.

A key to using silicon-based detectors at energies as high as 30 keV is making them thick. Fig. 4 shows the absorption efficiency of silicon of various thicknesses as a function of energy. Most commonly used silicon-based detectors have thicknesses of order 0.3 mm, which limits their efficiency at high energies. In order to obtain good efficiency at 20-30 keV, silicon thicknesses of 1–2 mm are required. However, in order to maintain efficient charge collection across the full thickness of the silicon, the material must be fully depleted. Fig. 5 shows the bias voltage required to fully deplete silicon of various resistivities versus silicon thickness. To fully deplete thick silicon detectors, high resistivity material is required and an electrode structure which can apply a high bias voltage to the silicon without resulting breakdown must be designed and fabricated.

There are several types of silicon X-ray detectors including P-I-N photodiodes, silicon strip detectors, silicon drift detectors, and avalanche photodiodes. These detectors differ in the geometry of the applied fields and the drift path of the charge carriers. Avalanche photodiodes include a region of high electric field in which the charge

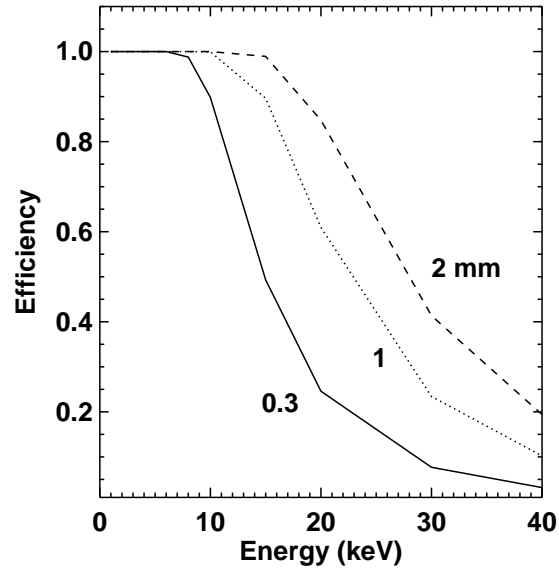


**FIGURE 4.** Absorption efficiency in silicon of various thicknesses versus incident photon energy.

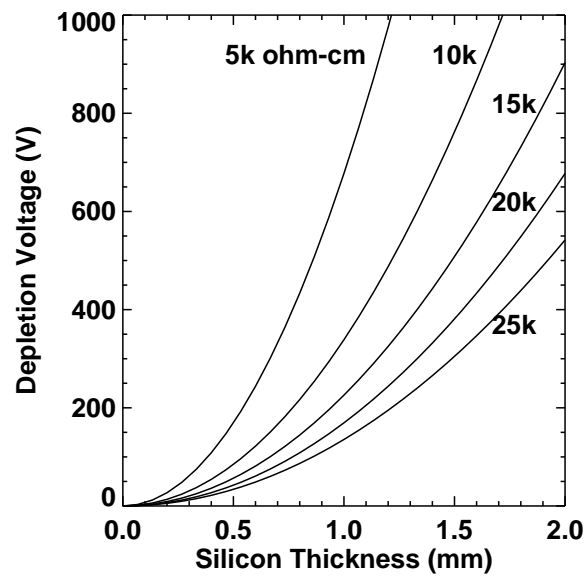


**FIGURE 5.** Bias voltage required to fully deplete silicon of various resistivities versus silicon thickness.

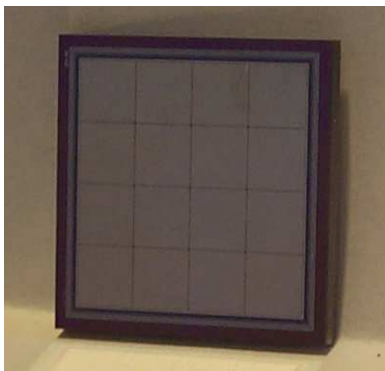


**FIGURE 6.** A  $4 \times 4$  array of silicon PIN photodiodes. Each is  $5 \text{ mm} \times 5 \text{ mm}$  in area and has a thickness of 1.5 mm.

carriers gain sufficient energy to cause charge multiplication. In the other detectors, there is no amplification of charge and low-noise electronics are required to detect the signals. Below, we briefly review the properties of and highlight recent work on the various types of silicon-based X-ray detectors.

### PIN Photodiodes

The simplest silicon detector is the PIN photodiode. At the Smithsonian Astrophysical Observatory (SAO), we have an active program to develop PIN photodiode X-ray detectors concentrating on producing devices with good performance in the 2–30 keV band. Much of our work to date has concentrated on the optimization of designs for thick devices. We have fabricated both single pixel devices and arrays of pixels.

As noted above, the key problem with thick silicon detectors is that a high bias voltage must be applied to fully deplete the silicon and allow efficient collection of the charge produced by incident X-rays. Many previous attempts to fabricate thick silicon detectors have failed because either the detectors break down when the bias voltage is applied or the bias required causes large dark currents, leading to poor performance. Success has been obtained for the thick PIN diodes for the hard X-ray instrument on Astro-E and now Astro-E2 [21].

Multi-guard ring structures allow high bias voltages to be applied without causing excessive dark currents or premature detector breakdown [11, 4, 10]. Working with Photon Imaging, Inc., we have designed new multi-guard ring structures which minimize the dead space around the active detector area and fabricated devices from thick silicon wafers with good efficiency up to 30 keV. The devices were fabricated from high resistivity silicon to lower the depletion voltage. The starting material was carefully selected and the pixel p/n junction diffusion

structures were optimized to further increase the breakdown voltage [26, 28, 6]. These advanced designs produced very low dark currents, leading to 1.5 mm thick detectors with good X-ray performance. A photograph of a  $4 \times 4$  array of  $25 \text{ mm}^2$  pixels is shown in Fig. 6.

Due to their large volume, and correspondingly large dark currents, these devices must be cooled to obtain good performance. We measured the response of 1.5 mm thick,  $25 \text{ mm}^2$  area diodes to X-rays emitted by the radioactive isotopes  $^{55}\text{Fe}$  and  $^{109}\text{Cd}$ . The X-ray response was measured with the diodes fully depleted at 500 V and cooled to  $-30^\circ\text{C}$ . A standard low noise NIM-based amplifier and a PC-based multi-channel analyzer were used for data collection. We obtained an energy resolution of 775 eV FWHM at 5.9 keV and 800 eV at 22 keV. This energy resolution meets the scientific requirements for a new X-ray timing mission.

### Silicon strip detectors

Silicon strip detectors differ from PIN photodiodes primarily in the geometry of the charge collection electrodes. Strip detectors typically have multiple electrodes arranged as strips on a single piece of silicon. The primary advantage of the strip layout is that it provides position sensing according to which strip collects the charge. Two dimensional position sensing is accomplished using strip patterns rotated by  $90^\circ$  on two sides of a single device. Strip detectors have been very actively developed by the high-energy particle physics community for use as charged particle trackers. The disadvantage of strips relative to PIN photodiodes for X-ray applications is that strips have higher capacitance and therefore higher noise than individual pixel devices or arrays of square or hexagonal pixels.

Silicon strip detectors are being used for the Super-Agile X-ray Telescope which is part of the Italian Agile Gamma-Ray mission [9]. The Super-Agile telescope is sensitive in the 10–40 keV band. The low energy limit of the telescope is primarily determined by the electronic noise of reading out the strips. Silicon strips are also being actively developed by the Naval Research Laboratory (NRL) for several applications (see the contribution by Philips in this volume). The NRL group has demonstrated an energy resolution of  $\Delta E < 1 \text{ keV}$  with  $16 \text{ mm}^2$  pixels and is currently fabricating large format detectors.

### Silicon drift detectors

In silicon drift detectors [14], the drift field is not uniformly perpendicular to the silicon surface, as is the case for PIN photodiodes and strip detectors and shown

in Fig. 3. Instead, the electric field within the silicon is shaped so that charge collected over a large volume within the silicon is transported to a relatively small collection anode. This leads to a greatly decreased anode capacitance and a corresponding decrease in electronic noise. An energy resolution of 250 eV for a 30 mm<sup>2</sup> device operated at a temperature of -20 C has been reported [12].

The disadvantage of silicon drift chambers is that they require electric field shaping electrodes to produce the needed internal electric field geometry. This makes the manufacture of drift chambers more complex than that of PIN photodiodes or silicon strip detectors. The field shaping also requires significantly more power than the simpler detectors. Finally, silicon drift chambers have not yet been successfully developed in thick configurations suitable for detection of X-rays up to 20–30 keV.

### Avalanche photodiodes

Avalanche photodiodes differ from all of the other types of silicon-based X-ray detectors in that they offer internal charge multiplication [17, 29]. The internal amplification is produced by introducing a second region within the silicon where the electric field is sufficiently high that charge carriers gain enough energy to ionize silicon between collisions with the silicon lattice. This eases issues concerning the very low noise electronics required for operation of any of the other types of silicon-based detectors in the standard X-ray band down to energies around 2 keV. However, the internal amplification is not perfectly linear. It is subject to fluctuations which reduce the energy resolution. Typical values for the energy resolution of avalanche photodiodes are  $\Delta E \sim 1.2$  keV at 6 keV, although resolution as good as  $\Delta E = 550$  eV at 6 keV has been reported recently [19]. Disadvantages of avalanche photodiodes are that their manufacture is complex and they have not been developed in thick configurations.

### CONCLUSION

Silicon-based detectors offer a potential means to realize the large area X-ray detector required for a new X-ray timing mission. At the current time, PIN photodiodes are sufficiently developed that they meet the basic requirements for a new timing mission and silicon strips should soon be demonstrated which meet the requirements. The main area of development required at present is in the production of the large number of low-noise, low-power electronics needed. Silicon-based detectors are robust and have a long heritage in space. The

detectors are low mass and no pressure vessel is needed. Silicon-based detectors can be mass produced in large quantities using well-proven and widely available techniques developed by the microelectronics industry.

The revolutionary advances of the Rossi X-Ray Timing Explorer opened a new window to relativistic gravity and the physics of extreme phenomena, which are central to NASA's scientific goals. Significant advances in our understanding of compact objects and accretion in strong gravitational fields are possible with a modest, dedicated X-ray timing mission.

### ACKNOWLEDGMENTS

This review is an updated version of one presented at COSPAR 2002 and available at astro-ph/0303421. I thank the Smithsonian Astrophysical Observatory for support of this work. I thank Steve Murray, Jeff McClintock, and Paul Gorenstein for useful discussions.

### REFERENCES

1. Abramowicz, M.A. and Kluzniak, W. 2001, *A&A*, 374, L19
2. Aschenbach et al. 2001, "X-ray Evolving Universe Spectroscopy - The XEUS Telescope", ESA document SP-1253
3. Aukerman, L.W., Vernon, F.L. Jr., and Song, L. 1984, *Opt. Eng.*, 23, 678
4. Avset, B.S., and Evensen, L. 1996, *NIM*, **A377**, 397
5. Barret, D. et al. 2001, *ApSSS*, 276, 305
6. Beck, G.A. et al. 1996, *NIM*, **A373**, 223
7. Berger, M. 1996, *ApJ*, 469, L13
8. Bradt, H.V. 1999, "Highlights from RXTE after 2.5 Years: Neutron-star Spins at KiloHertz Frequencies, Microquasars and More", in *Frontier Objects in Astrophysics and Particle Physics*, Proceedings of the Vulcano Workshop, Vulcano, Italy, May 1998, eds. F. Giovannelli & G. Mannoccihi, Societa' Italiana di Fisica, Editrice Compositori, Bologna, Italy; astro-ph/9901174
9. Costa, E. et al. 2001, in *X-Ray Astronomy: Stellar Endpoints, AGN, and the Diffuse X-ray Background*. Edited by Nicholas E. White, Giuseppe Malaguti, and Giorgio G.C. Palumbo. Melville, NY: American Institute of Physics, 2001. AIP Conf. Proc. 599, pp. 582-585
10. Da Rold, M. et al. 1997, *IEEE Trans. Nucl. Sci.*, 44, 721
11. Evensen, L. et al. 1993, *NIM*, **A337**, 44
12. Fiorini, C et al. 2001, *NIM*, **A458**, 281
13. Ford, E.C. 1999, *ApJ*, 519, L73
14. Gatti, E. & Rehak, P. 1984, *NIM*, **A255**, 608
15. Kaaret, P. et al. 1998, *ApJ*, qq
16. Kaaret, P. et al. 2001, *AIP Conf. Proc.*, 599, 678
17. McIntyre, R.J. 1966, *IEEE Trans. Electron Devices*, ED-13, 164
18. Morgan, E.H., Remillard, R.A., and Greiner, J. 1997, *ApJ*, 482, 993

19. Moszynski, M., Szawlowski, M., Kapusta, M., Balcerzyk, M. 2002, NIM, A485, 504
20. Muno, M.P., Fox, D.W., Morgan, E.H., and Bildsten, L. 2000, ApJ, 542, 1016
21. Ota, N. et al. 1999, NIM, A436, 291
22. Remillard, R.A. et al. 1999, ApJ, 517, L127
23. Strohmayer, T.E. et al. 1998, ApJ, 498, L135
24. Strohmayer, T.E. 2001, ApJ, 552, L49
25. Strohmayer, T.E. and Markwardt, C.B. 2002, ApJ, 577, 337
26. Sze, S.M. and Gibbons, G. 1966, *SSol. State Elect.*, 9, 831
27. Tananbaum, H. et al. 1972, ApJ, 174, L143
28. Waver, R.M. Jr. 1972, *SSol. State Elect.*, 15, 1303
29. Webb, P.P., McIntyre, R.J., Conradi, J. 1966, *RCA Review*, 27, 164